Near-Edge X-ray Absorption Fine Structure Spectroscopy Study of the Photolytic Process in Poly(phenyl thioether) with Pendant Iron Moieties

Edwige Otero,[†,§] Patrick O. Shipman,[‡] Alaa S. Abd-El-Aziz,[*,‡] and Stephen G. Urquhart[*,†]

Department of Chemistry, University of Saskatchewan, 110 Science Pl., Saskatoon, Saskatchewan S7N 5C9, Canada, and Department of Chemistry, University of British Columbia Okanagan, Kelowna, British Columbia V1V 1V7, Canada

Received August 9, 2008; Revised Manuscript Received November 7, 2008

ABSTRACT: The near-edge X-ray absorption fine structure (NEXAFS) spectra of poly(phenyl thioether) polymers with pendant Fe(Cp) iron moieties have been recorded at the carbon 1s, iron 2p, and phosphorus 1s and 2p edges. This study shows that solution photofragmentation of the organometallic polymer causes the removal of iron moieties and the preparation of the corresponding organic polymer: poly(phenyl thioether). Spectroscopic characterization of poly(phenyl thioether) prepared in this manner indicates the presence of iron oxide, likely Fe_2O_3, and hexafluorophosphate counterion trapped in the demetalated polymer matrix. A photolytic examination of the solid phase poly(phenyl thioether)−Fe(Cp) organometallic polymer shows that irradiation of this polymer in air leads to the formation of poly(phenyl thioether) and Fe_2O_3, while irradiation in vacuum leads to formation of iron species with a lower oxidation state. The ability to probe the oxidation state of this metal species is relevant to understanding how demetalation conditions affect the properties of the polymer.

1. Introduction

The incorporation of transition metal species into polymers is an effective method for controlling and optimizing the electric, magnetic, optical, redox, and mechanic properties of these polymers as well as their processability, particularly their solubility.[1−4] The reaction of Fe(Cp)(1,*n*-dichlorobenzene) where $n = 2$, 3, or 4 and Cp = cyclopentadienyl, with various oxygen and sulfur dinucleophiles, leads to the synthesis of soluble cyclopentadienyliron functionalized polymers containing aromatic ether, thioether, and amine bridges with relatively high molecular weight.[5−8]

The preparation of organic materials such as polyphenylene sulfide, a thermoplastic widely used in the polymer industry, traditionally requires extreme conditions. The synthesis of polyphenylene sulfide suffers from a relatively mediocre yield and the poor solubility of the polymer, leading to low molecular weight. An alternative route to the synthesis of polyphenylene sulfide has been proposed by Abd El Aziz et al. via photolytic demetalation of cyclopentadienyliron functionalized poly(phenylene sulfide). This process, performed at room temperature, was found very efficient in preparing polyethers and polythioethers with high molecular weight in yields greater than 70%.[8]

The photolysis of metal arene monomers (i.e., $[(Cp)Fe(Bz)^+][X^-]$ where X^-, the counterion = PF_6^-, BF_4^-, AsF_6^-, SbF_6^-, BPh_4^-) and substituted derivatives has been extensively investigated due to the use of the cation as a polymerization photoinitiator.[9] The mechanism, intermediates, and products formed during the photodearylation of $[(Cp)Fe(Bz)^+][X^-]$ in solution have been examined using nuclear magnetic resonance,[10,11] infrared spectroscopy,[10−12] UV−vis spectroscopy,[10,13−17] fluorescence spectroscopy,[12,18] conductivity measurements,[14,15] electrochemistry,[19] time-resolved laser spectroscopy,[20] high-pressure liquid chromatography and gas chromatography−mass spectroscopy,[12] and electron spray ionization mass spectroscopy.[21,22] The reaction is affected by the nature of the substituents on either the benzene or cyclopentadiene rings, the polarity of the solvent, the identity of the counterion, the excitation wavelength, and the temperature. From these studies, a general mechanism was suggested: excitation of either $[(Cp)Fe(Bz)^+][X^-]$ or freely solvated cation $(Cp)Fe(Bz)^+$ causes arene ring slippage from η^6-Bz to η^4-Bz followed by replacement of the arene by three ligands to form $[(Cp)Fe(L)_3^+][X^-]$.[23] The unstable trisubstituted intermediate eventually decomposes into either ferrocene, iron metal, or some other species containing iron, a counterion, and solvent molecules. On the other hand, the investigation of the photolytic demetalation process of cyclopentadienyliron functionalized polymers remains quite unclear. Formation of ferrocene and iron metal during the photolytic process in solution has been observed, and the presence of unidentified impurities trapped in trace amounts within the organic polymer will affect the properties of the organic polymer. The incorporation of transition metal containing nanoparticles into the organic matrix is of interest for preparing magnetic ceramic materials; the photolysis of organometallic polymers was recently proven useful for such applications.[24,25]

In this article, we present the NEXAFS spectroscopy of poly(phenyl thioether) with pendant iron moieties and poly(phenyl thioether) prepared by demetalation of the organometallic polymer in solution (cf. Scheme 1). Impurities present in poly(phenyl thioether) are identified as high-spin $3d^5$ iron species, likely iron oxides, along with the PF_6^- counterion. The same remnant iron species were obtained after solid-state photolysis in solution or in air, while solid-state photolysis in vacuum leads to the formation of different iron remnant species, likely an Fe(II) species.

2. Experimental Section

2.1. Reagents and Sample Preparation. *Reagents.* Poly[thio(η^6-1,4-phenylene)thio-1,4-phenylthio-1,4-phenylene(η^5-cyclopentadienyl)iron(II)] hexafluorophosphate (PPS-$[Fe(Cp)^+][PF_6^-]$) was

---

[*] Corresponding authors. E-mail: stephen.urquhart@usask.ca; alaa.abd-el-aziz@ubc.ca.
[†] University of Saskatchewan.
[‡] University of British Columbia Okanagan.
[§] Current address: Synchrotron SOLEIL, L'Orme des Merisiers Saint-Aubin, BP 48 91192 Gif-sur-Yvette Cedex, France.

10.1021/ma801826p CCC: $40.75

Scheme 1. Chemical Structures of [(Cp)Fe(Bz-S-Ph)$^+$][PF$_6^-$] (Single Repeat Unit of the PPS−[Fe(Cp)$^+$][PF$_6^-$] Polymer, a.k.a. Monomer), PPS−[Fe(Cp)$^+$][PF$_6^-$] (a.k.a. Metalated Polymer), and PPS (a.k.a. Demetalated Polymer)

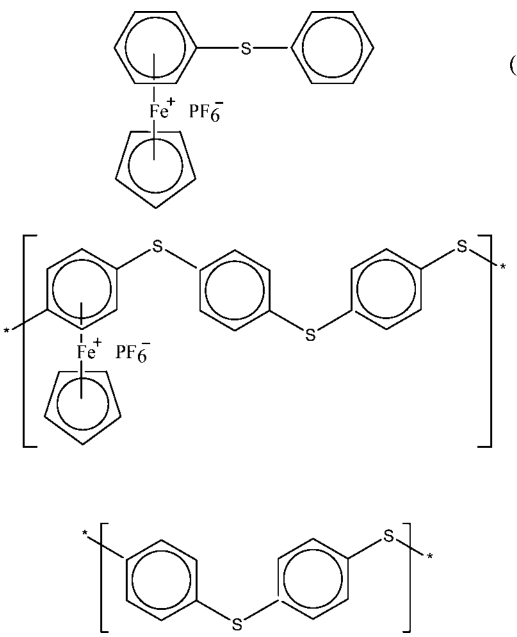

(η^6-1,1'-thiobisbenzene)(η^5-cyclopentadienyl)
iron(II) hexafluorophosphate
[(Cp)Fe(Bz-S-Ph)][PF$_6$]

poly[thio(η^6-1,4-phenylene)thio-1,4-phenylthio-
1,4-phenylene(η^5-cyclopentadienyl)
iron(II) hexafluorophosphate
PPS-[Fe(Cp)][PF$_6$]

poly(phenyl thioether)
PPS

Table 1. Preparation Conditions for Irradiated and Nonirradiated Poly(phenyl thioether) (PPS) and Metalated, PPS−[Fe(Cp)$^+$][PF$_6^-$] Polymer Samples

compound	preparation	UV light source	conditions	referred to as
poly(phenyl thioether) (PPS)	photolytic demetalation of PPS−[Fe(Cp)$^+$][PF$_6^-$] in acetonitrile; sample consisted of black hard chips; ground and pressed into indium, carbon tape, or copper substrates	Rayonet Mini-Reactor at a wavelength of 2537 Å	N$_2$ atmosphere	in-solution demetalated polymer
PPS−[Fe(Cp)$^+$][PF$_6^-$]	as-received powder pressed into indium, carbon tape, and copper	nonirradiated	N/A	as-received metalated polymer
	metalated polymer film; cast from a filtered DMF solution onto gold-coated silicon	nonirradiated	N/A	filtered metalated polymer
PPS + Fe species + PF$_6^-$ residues	photolysis of the PPS−[Fe(Cp)$^+$][PF$_6^-$] film; film was cast onto Au-coated Si wafer from filtered solution in DMF	mercury arc lamp (100 W, Newport model 6281)	in air	method 1: irradiated in air
	photolysis of PPS−[Fe(Cp)$^+$][PF$_6^-$] film; film was cast onto Au-coated Si wafer from filtered solution in DMF	nnmonochromatized synchrotron radiation	in vacuum	method 2: irradiated in vacuum
	photolysis of PPS-[Fe(Cp)$^+$][PF$_6^-$] film; film was cast onto Au-coated Si wafer from filtered solution in DMF	mercury arc lamp (100 W, Newport model 6281)	in vacuum	method 3: irradiated in vacuum

prepared according to published procedures.[5,8] All compounds except dimethylformamide and potassium hexacyanoferrate were obtained from Aldrich. Iron(III) oxide (Fe_2O_3, >99%), sodium pyrophosphate ($Na_4P_2O_7$, >99%), sodium hexafluorophosphate ($NaPF_6$, >99%), urea (NH_2CONH_2, 99%), and potassium hexacyanoferrate ($K_4[Fe(CN)_6]$, >99%, purchased from BDH) were used without further purification. Dimethylformamide (DMF, neat) was freshly distilled on the day of the sample preparation. The NEXAFS spectra of [(Cp)Fe(Bz-S-Ph)$^+$][PF$_6^-$], a single repeat unit of the PPS−[Fe(Cp)$^+$][PF$_6^-$] polymer, was reproduced from the literature.[26]

Poly(phenyl thioether) (PPS) was prepared by photolytic demetalation of PPS−[Fe(Cp)$^+$][PF$_6^-$] in solution, performed by Abd-El-Aziz et al. using a Rayonet Mini-Reactor at a wavelength of 2537 Å.[8] This demetalated PPS sample formed black, hard chips and was used without further purification. Molecular structures of materials studied are presented in Scheme 1.

Several different methods were used to prepare irradiated and nonirradiated samples of poly(phenyl thiolether) and PPS−[Fe(Cp)$^+$][PF$_6^-$] polymers; these methods are summarized in Table 1. Solid samples of PPS−[Fe(Cp)$^+$][PF$_6^-$] and solution-demetalated PPS were prepared by pressing milligram amounts of each compound into either indium foil (0.25 mm thick, 99.99% purity, Aldrich), conductive carbon tape (Structure Probe Inc.), or solid copper substrates (MDC Vacuum). Substrates were selected for experimental ease and the absence of the element under study; these are listed for each spectrum in the figure captions. Films of PPS−[Fe(Cp)$^+$][PF$_6^-$] were also prepared by casting filtered solutions of the compounds in dimethylformamide (DMF) onto gold-coated silicon wafers. The filtration of PPS$-$[Fe(Cp)$^+$][PF$_6$$^-$] polymer solution was used to remove potential residues formed by degradation of the metalated polymer following the synthesis. Unfiltered and filtered samples will be referred to as "as-received" and "filtered" samples, respectively, throughout the text and figure captions.

Solid-state photolysis was performed using three different methods: photolysis in air, using mercury arc lamp (Oriel 60000 series Q housing with 100 W mercury arc lamp, Newport model 6281); photolysis in vacuum, using unmonochromatized synchrotron radiation ("white light") and photolysis in vacuum, using an external mercury-arc lamp and a UV transparent sapphire window (MDC Vacuum, VP100S).

Great care was taken during sample preparation and storage to protect the films from unwanted light exposure and photofragmentation. To determine the effectiveness of this method, a series of as-received (i.e., without solution filtration) metalated polymer samples were examined by pressing milligram amount of the powder into indium foil and carbon tape. These samples are referred to as "as-received" PPS$-$[Fe(Cp)$^+$][PF$_6$$^-$] powder samples.

2.2. Measurements. All NEXAFS spectra presented here were obtained by recording the sample current in total electron yield (TEY) mode. Phosphorus 2p and sulfur 2p NEXAFS spectra were collected using the Canadian Synchrotron Radiation Facility Mark IV beamline then on port 091 at the Synchrotron Radiation Center (University of Wisconsin, United States). The Mark IV beamline uses a "Grasshopper"-type grazing incidence Brown-Lien-Pruett grating monochromator and covers the photon energy range 21$-$1000 eV.[27] The spectroscopic resolving power ($E/\Delta E$) is estimated as better than 1200.[27] The iron 2p and carbon 1s edge NEXAFS spectra were obtained using the spherical grating monochromator (SGM) beamline 11-ID.1 at the Canadian Light Source (University of Saskatchewan, Canada). This beamline is equipped with a Dragon-type spherical grating monochromator and was designed for high-resolution soft X-ray spectroscopy studies.[28] The spectroscopic resolving power ($E/\Delta E$) is estimated as better than 3200. Phosphorus and sulfur 1s NEXAFS spectra were recorded using the Canadian double-crystal monochromator (DCM) beamline on port 093 at the Synchrotron Radiation Center (University of Wisconsin).[29] The DCM uses a Golovchenko-type boomerang mechanism and covers the energy range 1500$-$4000 eV with a spectroscopic resolving power estimated as better than 2300.

The spectra recorded at phosphorus and sulfur 1s and 2p edges were normalized according to the following equation:

$$\text{normalized spectra} = [I/I_0] \tag{1}$$

where I corresponds to the sample current and I_0 to the current from a mesh monitor located upstream of the sample. Iron 2p edge spectra were normalized using the double-normalization method:

$$\text{normalized spectra} = [I/I_0]/[I_R/I_{0R}] \tag{2}$$

where I_R and I_{0R} correspond to the reference sample and mesh currents recorded from a gold-coated silicon wafer or clean indium foil. At the carbon edge, spectra were normalized by the following equation:

$$\text{normalized spectra} = [I]/[I_R] \tag{3}$$

where I_R corresponds to the reference sample current recorded from a gold-coated silicon wafer or clean indium foil. The normalization processes was described is detail previously.[30]

Relative energy scale calibration at phosphorus 2p$-$sulfur 2p edges was obtained by recording the NEXAFS spectrum of silicon dioxide at silicon 2p edge. The presence of a native oxide layer on the surface of the silicon wafer is characterized by a strong absorption peak observed at 108.04 eV by Sutherland et al.[31] and assigned to silicon 2p → t_2 transition in SiO$_2$ by Li et al.[32] The energy scale at carbon 1s edge was calibrated relative to the carbon 1s NEXAFS spectrum of urea in solid phase. In gas phase urea is characterized by a strong and narrow absorption peak assigned to the carbon 1s → π^*(C=O) transition and reported at 289.53 eV by Urquhart et al., after an ISEELS absolute energy scale calibration.[33] The iron 2p edge spectra were calibrated relative to the lowest energy feature in the iron 2p NEXAFS spectrum of K$_4$[Fe(CN)$_6$]. This feature was observed at 710.25 eV by Otero et al., after energy scale calibration against SF$_6$(g).[30] Phosphorus 1s NEXAFS spectra were calibrated relative to the main feature in Na$_4$P$_2$O$_7$ spectrum observed by Engemann et al. at 2152.4 eV.[34]

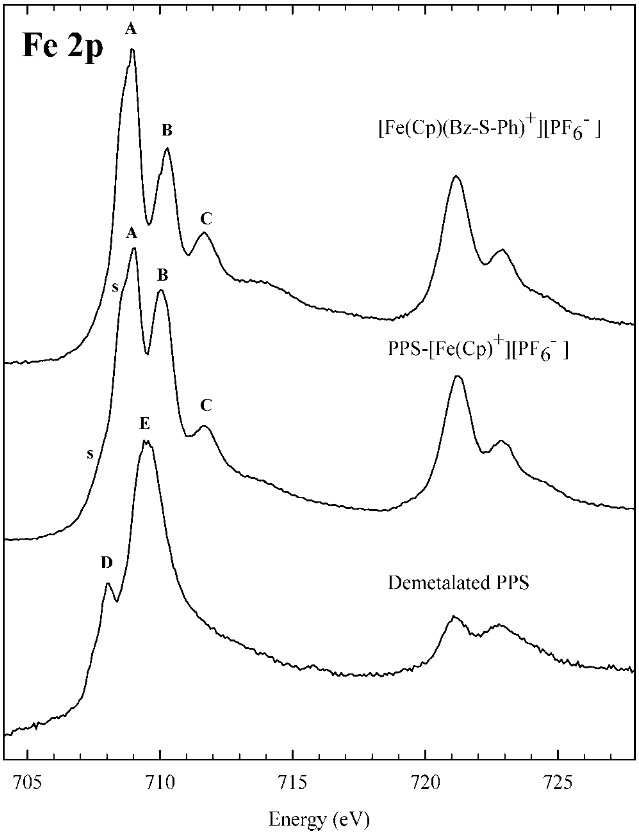

Figure 1. Iron 2p NEXAFS spectra of [(Cp)Fe(Bz-S-Ph)$^+$][PF$_6$$^-$] monomer, reproduced from ref 26 (sample embedded into an indium metal substrate), the metalated polymer film (PPS$-$[Fe(Cp)$^+$][PF$_6$$^-$] (cast from a filtered DMF solution onto gold-coated silicon), and the iron residue present in demetalated PPS (embedded into an indium metal substrate), prepared by solution photolytic demetalation of PPS$-$[Fe(Cp)$^+$][PF$_6$$^-$]. The spectra have been offset by a constant for clarity.

3. Results

3.1. Characterization of Metalated and Demetalated Polymers. *3.1.1. Iron 2p Edge NEXAFS Spectra.* Figure 1 presents the iron 2p NEXAFS spectra of [(Cp)Fe(Bz-S-Ph)$^+$][PF$_6$$^-$] monomer, reproduced from ref 26, PPS$-$[Fe(Cp)$^+$][PF$_6$$^-$] metalated polymer film, filtered and cast from DMF, and demetalated PPS, prepared by solution photolytic demetalation of PPS$-$[Fe(Cp)$^+$][PF$_6$$^-$]. The spectra have been offset by a constant for clarity. Transition energies and assignments for these compounds are presented in Table 2. Features observed above 718 eV correspond to transitions from iron 2p$_{1/2}$ edge and resemble those observed below 714 eV, which correspond to transitions from iron 2p$_{3/2}$ edge. The following discussion will focus on the iron 2p$_{3/2}$ edge for which a better resolution was achieved.

The iron 2p NEXAFS spectrum of [(Cp)Fe(Bz-S-Ph)$^+$][PF$_6$$^-$] has been described previously.[26] The iron 2p spectrum PPS$-$[Fe(Cp)$^+$][PF$_6$$^-$] resembles that of its monomer unit, [(Cp)Fe(Bz-S-Ph)$^+$][PF$_6$$^-$]; it is characterized by a strong feature

Table 2. Transition Energies (eV) and Assignment for Iron 2p NEXAFS Spectra of [(Cp)Fe(Bz-S-Ph)$^+$][PF$_6^-$] Monomer, the Metalated Polymer, PPS−[Fe(Cp)$^+$][PF$_6^-$], and the Demetalated Polymer, PPS, Prepared by Solution Photolytic Demetalation

peak labels	[(Cp)Fe(Bz-S-Ph)$^+$][PF$_6^-$] (monomer)	PPS−[Fe(Cp)$^+$][PF$_6^-$]	PPS	assignment
s		707.5, 708.5		sample damage
D			708.16	
A	708.96	709.01		Fe 2p$_{3/2}$ → Fe 3d$_{xz}$/$\pi_{(Bz/Cp)}$ Fe 2p$_{3/2}$ → Fe 3d$_{yz}$/$\pi_{(Bz/Cp)}$
E			709.63	
B	710.28	710.06		Fe 2p$_{3/2}$ → $\pi^*_{(Bz)}$/Fe 3d Fe 2p$_{3/2}$ → $\pi^*_{(Bz-S)}$/Fe 3d
C	711.67	711.69		Fe 2p$_{3/2}$ → $\pi^*_{(Cp)}$/Fe 3d
	721.18	721.26	721.15	Fe 2p$_{1/2}$ → Fe 3d$_{xz}$/$\pi_{(Bz/Cp)}$ Fe 2p$_{1/2}$ → Fe 3d$_{yz}$/$\pi_{(Bz/Cp)}$
	722.9	722.8	722.8	Fe 2p$_{1/2}$ → $\pi^*_{(Bz)}$/Fe 3d Fe 2p$_{1/2}$ → $\pi^*_{(Bz-S)}$/Fe 3d
	724.5 broad	724.5 broad		

A observed at 709.0 eV followed by two weaker features, B at ~710.0 eV and C at 711.7 eV. Note the presence of shoulders (s) on the low-energy side of A. The intensity of these shoulders increases as spectra are recorded successively from the same sample area. This indicates that PPS−[Fe(Cp)$^+$][PF$_6^-$] is sensitive to radiation damage, and these shoulders are so assigned.

The strong iron 2p signal from the demetalated PPS polymer at first seems surprising, except that we are examining the iron residue left from the solution demetalation process. The spectrum of the iron residue trapped in demetalated PPS differs considerably from the spectra of PPS−[Fe(Cp)$^+$][PF$_6^-$]. The iron residual spectrum is dominated by a high-energy feature E at 709.63 eV and a weaker feature D at 708.16 eV (see Figure 1).

Figure 2 presents the iron 2p NEXAFS spectrum of the metalated polymer film (PPS−[Fe(Cp)$^+$][PF$_6^-$], cast from a filtered DMF solution (reproduced from Figure 1)) and spectra of the as received PPS−[Fe(Cp)$^+$][PF$_6^-$] powder sample, recorded at two different locations. The spectra recorded from the as-received PPS−[Fe(Cp)$^+$][PF$_6^-$] powder sample are significantly different from the spectrum collected from the filtered PPS−[Fe(Cp)$^+$][PF$_6^-$] sample. Spectra recorded at different locations on the powder sample are inconsistent, indicating that the as-received PPS−[Fe(Cp)$^+$][PF$_6^-$] powder sample contains inhomogeneous impurities, likely photolysis residues.

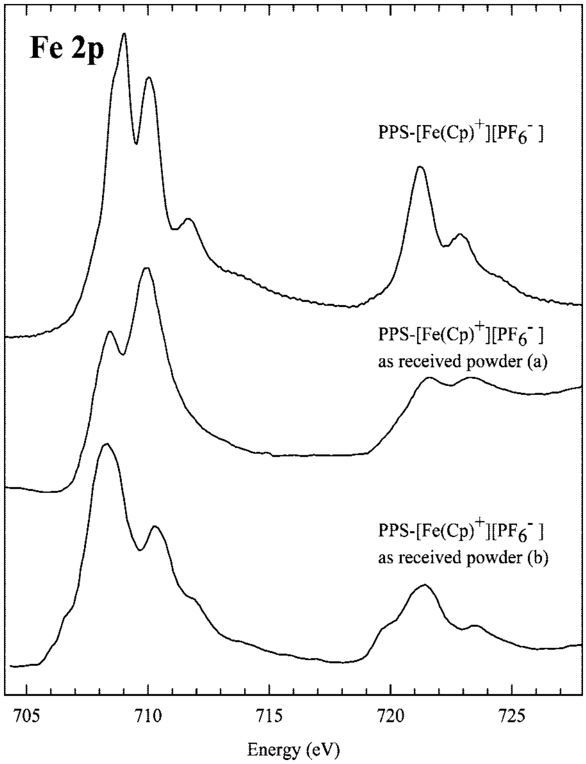

Figure 2. Iron 2p edge NEXAFS spectra of the metalated polymer, PPS−[Fe(Cp)$^+$][PF$_6^-$] (cast from a filtered DMF solution onto gold-coated silicon), and the spectra from two locations (a, b) of the as-received, unfiltered PPS−[Fe(Cp)$^+$][PF$_6^-$] powder sample (embedded into indium metal). The spectra have been offset by a constant for clarity.

3.1.2. C 1s edge NEXAFS spectra. The carbon 1s NEXAFS spectra of [(Cp)Fe(Bz-S-Ph)$^+$][PF$_6^-$] (reproduced from ref 26), a PPS−[Fe(Cp)$^+$][PF$_6^-$] film cast from filtered DMF solution, and the demetalated polymer, PPS, prepared by photolytic demetalation in solution of PPS−[Fe(Cp)$^+$][PF$_6^-$]) are presented Figure 3. The transition energies and assignments for these compounds are presented in Table 3.

The spectrum of the monomer unit, [(Cp)Fe(Bz-S-Ph)$^+$]-[PF$_6^-$], described previously,[26] resembles that of metalated polymer, PPS−[Fe(Cp)$^+$][PF$_6^-$]. The spectra of the monomer and polymer are dominated near 284.9 eV by a strong feature A followed by a shoulder A′. Peak B, observed distinctively at 286.04 eV in the spectrum of [(Cp)Fe(Bz-S-Ph)$^+$][PF$_6^-$], is barely visible on the spectrum of PPS−[Fe(Cp)$^+$][PF$_6^-$]. Similarly, the intensity of peak C observed at 287.05 eV in the spectrum of [(Cp)Fe(Bz-S-Ph)$^+$][PF$_6^-$] decreases somewhat in the spectrum of PPS−[Fe(Cp)$^+$][PF$_6^-$]. The spectrum of the demetalated PPS prepared by solution photolysis is dominated by an intense feature A at 284.94 eV followed by a well-resolved shoulder A′. Weak peaks C, D′, D, and E are observed above 287 eV. Note the absence of feature in the energy range 285.5−286.5 eV.

3.1.3. Phosphorus 1s Edge NEXAFS Spectra. The phosphorus 1s NEXAFS spectra of the [(Cp)Fe(Bz-S-Ph)+][PF$_6^-$] monomer, the PPS−[Fe(Cp)$^+$][PF$_6^-$] film cast from a filtered DMF solution, the demetalated polymer (PPS) prepared by solution photolytic demetalation of PPS−[Fe(Cp)$^+$][PF$_6^-$]), NaPF$_6$, and the as-received PPS−[Fe(Cp)$^+$][PF$_6^-$] powder sample are presented in Figure 4. NaPF$_6$ acts as a model for the PF$_6^-$ counterion, the PPS sample contains some residual PF$_6^-$ counterion, and the comparison of the as-received powder and the filtered PPS−[Fe(Cp)$^+$][PF$_6^-$] samples show the effect of impurities in the metalated PPS polymer.

The spectra of the [(Cp)Fe(Bz-S-Ph)$^+$][PF$_6^-$] monomer, the solution filtered PPS−[Fe(Cp)$^+$][PF$_6^-$] polymer, the demetalated PPS sample, and the NaPF$_6$ model are dominated by a strong peak observed at 2157.9 eV. This is preceded by a weak shoulder at 2153.4 eV. The intensity of this low-energy feature increases in the spectrum of the filtered PPS−[Fe(Cp)$^+$][PF$_6^-$] sample and in the demetalated PPS sample. The spectrum of the as-received PPS−[Fe(Cp)$^+$][PF$_6^-$] powder sample shows

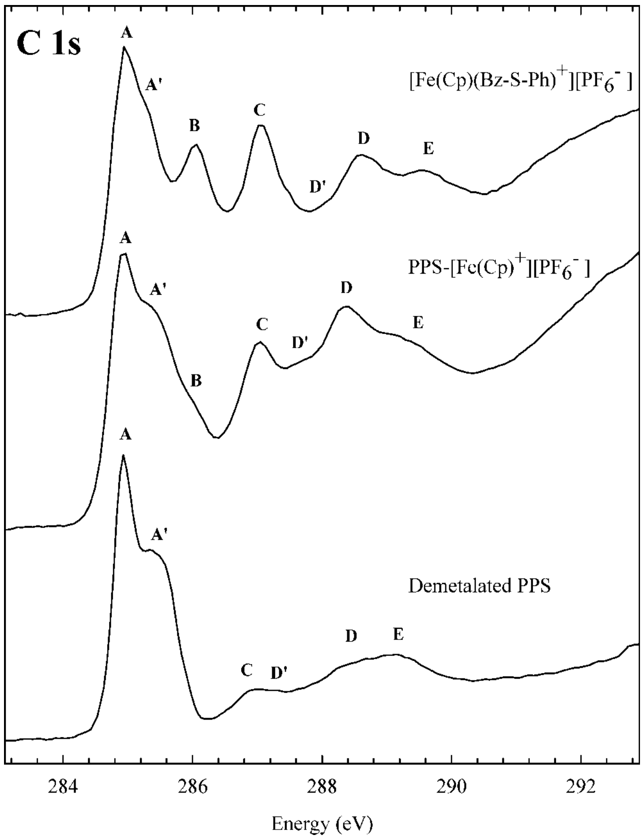

Figure 3. Carbon 1s edge NEXAFS spectra of [(Cp)Fe(Bz-S-Ph)$^+$][PF$_6^-$] monomer (embedded in indium metal), PPS−[Fe(Cp)$^+$][PF$_6^-$] film (cast from filtered DMF solution onto gold-coated silicon), and PPS from the solution photolytic demetalation of PPS−[Fe(Cp)$^+$][PF$_6^-$]) (embedded in indium metal). The spectra have been offset by a constant for clarity.

two features at 2152.64 and 2157.66 eV, with the second peak slightly more intense than the former.

3.1.4. Phosphorus 2p Edge and Sulfur 2p Edge NEXAFS Spectra. The phosphorus 2p and sulfur 2p NEXAFS spectra of the [(Cp)Fe(Bz-S-Ph)$^+$][PF$_6^-$] monomer, the PPS−[Fe(Cp)$^+$]-[PF$_6^-$] film (prepared from a filtered DMF solution), the demetalated PPS, and the NaPF$_6$ model are presented in Figure 5. Transition energies and assignments are presented in Table 4. Features observed at low energy (135−163 eV) correspond to phosphorus 2p edge transitions, while features at higher energy (163−175 eV) correspond to sulfur 2p edge transitions. Peak J observed at ~201.3 eV in the spectra of NaPF$_6$, [(Cp)Fe(Bz-S-Ph)$^+$][PF$_6^-$], and PPS−[Fe(Cp)$^+$][PF$_6^-$] is assigned as a phosphorus 2s transition. The spectra of [(Cp)Fe(Bz-S-Ph)$^+$][PF$_6^-$], PPS−[Fe(Cp)$^+$][PF$_6^-$], and NaPF$_6$ are similar at the phosphorus 2p edges, except for a weak shoulder a′ observed on the low-energy side of peak A in the spectra of PPS−[Fe(Cp)$^+$][PF$_6^-$] and NaPF$_6$. The spectra of [(Cp)Fe(Bz-S-Ph)$^+$][PF$_6^-$], PPS−[Fe(Cp)$^+$][PF$_6^-$], and PPS (+ PF$_6^-$ residue) show similar features at sulfur 2p edges. A decrease in intensity of the resonances at phosphorus 2p edges compared to sulfur 2p edges is observed in the spectrum of PPS−[Fe(Cp)$^+$][PF$_6^-$] relative to the spectrum of [(Cp)Fe(Bz-S-Ph)$^+$][PF$_6^-$], and only very discrete features at 139.04 eV, 149.58, and 162.2 eV are present in the PPS (+ PF$_6^-$ residue) spectrum.

3.2. Photolytic Demetalation of PPS−[Fe(Cp)$^+$][PF$_6^-$] in Solid State. *3.2.1. Photolytic Study at Iron 2p Edge.* The first photolytic study of metalated polymer was performed on PPS−[Fe(Cp)$^+$][PF$_6^-$] films prepared by casting filtered DMF solutions. These samples were exposed to an Hg-arc lamp in air, for various amounts of time (irradiation method 1). The iron 2p NEXAFS spectra of these PPS−[Fe(Cp)$^+$][PF$_6^-$] films, before and after UV irradiation, are presented in Figure 6, in comparison to the spectrum of demetalated PPS polymer (prepared by solution photolytic demetalation of PPS−[Fe(Cp)$^+$][PF$_6^-$]) and Fe$_2$O$_3$. Transition energies are reported in Table 5.

The spectra of PPS−[Fe(Cp)$^+$][PF$_6^-$] films irradiated for few seconds show clear changes: presence of a weak and narrow feature a (at ~706.2 eV), intense shoulders on the low-energy side of feature A, a decrease in the intensity of feature A, and the disappearance of feature C. The spectra of PPS−[Fe(Cp)$^+$][PF$_6^-$] films irradiated for more than 1 min, demetalated PPS (+ iron residue), and Fe$_2$O$_3$ are characterized by the presence of a peak D near 708.1 eV followed by an intense feature E near 709.7 eV.

A second photolytic study was performed by in vacuum irradiation of PPS−[Fe(Cp)$^+$][PF$_6^-$] films prepared by casting filtered DMF solutions of the polymer. Unmonochromatized synchrotron light ("white light") was used (method 2). Figure 7 presents fluorine 1s and iron 2p NEXAFS spectra of PPS−[Fe(Cp)$^+$][PF$_6^-$] films recorded before and after irradiation for various amounts of time. Spectral features observed between 685 and 703 eV correspond to transition from F 1s edge and features observed above 703 eV to transitions from iron 2p edges (see Table 5 for transition energies observed at iron 2p edge). A decrease in intensity of fluorine 1s edge resonances is observed as the irradiation dose increases. After 150 s of irradiation the iron 2p$_{3/2}$ spectrum of PPS−[Fe(Cp)$^+$][PF$_6^-$] film is characterized by a strong features F observed at 707.81 eV followed by two weak peaks G and H at 710.21 and 711.48 eV.

A third photolytic study was performed in vacuum using a Hg-arc lamp (method 3, not shown here). In order to expose the metalated polymer film to the UV lamp, the sample needed to be moved between the spectroscopic measurement position and the UV exposure position, located behind a UV transparent sapphire window on the vacuum chamber. The irreproducible positioning of the sample between exposures affected the quality and reliability of the spectra. Despite these uncertainties, the same iron 2p spectral features were observed after 25 min irradiation with the Hg-arc lamp as were observed after 150 s of irradiation with synchrotron white light. The time differences could be attributed to the lower flux and different spectral distribution of the Hg arc lamp.

3.2.2. Photolytic Study at Carbon 1 s Edge. The carbon 1s NEXAFS spectrum of PPS−[Fe(Cp)$^+$][PF$_6^-$] film irradiated with Hg-arc lamp in air is presented in Figure 8 along with the unexposed PPS−[Fe(Cp)$^+$][PF$_6^-$] film and demetalated PPS spectra reproduced from Figure 3. Both PPS−[Fe(Cp)$^+$][PF$_6^-$] films were cast from filtered DMF solutions; the PPS polymer was prepared by solution photolytic demetalation.

The spectrum of irradiated PPS−[Fe(Cp)$^+$][PF$_6^-$] film is dominated by an intense low-energy peak A observed at 284.94 eV followed by a shoulder A′. Weaker and broad features (C) are observed around 287 eV followed by an intense peak F observed at 288.47 eV. Note the absence of peaks in the energy range 285.5−286.5 eV. Figure 9 presents the carbon 1s NEXAFS spectra of PPS−[Fe(Cp)$^+$][PF$_6^-$] film irradiated with unmonochromatized synchrotron light in vacuum for 1 min and for 30 min; transition energies for the 30 min irradiation spectrum are reported in Table 6. The spectra of PPS−[Fe(Cp)$^+$][PF$_6^-$] film (nonirradiated) and PPS reproduced from Figure 3 are presented for comparison. The spectra of PPS−[Fe(Cp)$^+$][PF$_6^-$] film irradiated for 30 min becomes

Table 3. Transition Energies (eV) and Assignment for Carbon 1s NEXAFS Spectra of the [(Cp)Fe(Bz-S-Ph)$^+$][PF$_6^-$] Monomer, the Metalated Polymer, PPS−[Fe(Cp)$^+$][PF$_6^-$], and the Demetalated Polymer, PPS, Prepared by Solution Photolytic Demetalation

peak labels	[(Cp)Fe(Bz-S-Ph)$^+$][PF$_6^-$]	PPS−[Fe(Cp)$^+$][PF$_6^-$]	assignment	PPS	assignment
A	284.96	284.94	Cp C $1s_{(C-H)} \rightarrow$ Fe $3d_{xz}/\pi_{(Cp)}$ Cp C $1s_{(C-H)} \rightarrow$ Fe $3d_{yz}/\pi_{(Cp)}$ Ph C $1s_{(C-H)} \rightarrow \pi^*_{(Ph-S)}$	284.94	Bz C $1s_{(C-H)} \rightarrow \pi^*_{(Bz)}$
A′	285.23 shoulder	285.32	Bz C $1s_{(C-H)} \rightarrow$ Fe $3d_{xz}/\pi^*_{(Bz/Cp)}$ Bz C $1s_{(C-H)} \rightarrow$ Fe $3d_{yz}/\pi^*_{(Bz/Cp)}$	285.36	Bz C $1s_{(Csub)} \rightarrow \pi^*_{(Bz-S)}$
B	286.04	286.0	Bz C $1s_{(Csub)} \rightarrow$ Fe $3d/\pi^*_{(Bz/Cp)}$ Bz C $1s_{(C-H)} \rightarrow \pi^*_{(Bz-S)}$/Fe 3d Ph C $1s_{(Csub)} \rightarrow \pi^*_{(Ph-S)}$		
C	287.05	287.06	Bz C $1s_{(sub)} \rightarrow \pi^*_{(Bz)}$/Fe 3d Cp C $1s_{(C-H)} \rightarrow \pi^*_{(Cp)}$/Fe 3d Ph C $1s_{(Csub)} \rightarrow \sigma^*_{(C-S)}$	287	Bz C $1s_{(Csub)} \rightarrow \sigma^*_{(C-S)}$
D′	287.5 sh	287.6	Bz C $1s_{(Csub)} \rightarrow \sigma^*_{(C-S)}$	287.75	Bz C $1s_{(Csub)} \rightarrow \sigma^*_{(C-S)}$ Bz C $1s_{(C-H)} \rightarrow \sigma^*_{(C-H)}$
D	288.62	288.40	Bz, Ph C $1s_{(Csub)} \rightarrow \sigma^*_{(C-S)}$ Cp, Bz, Ph C $1s_{(C-H)} \rightarrow \sigma^*_{(C-H)}$ Bz C $1s_{(C-H)} \rightarrow \pi^*_{(Bz-S)}$	288.5	Bz C $1s_{(C-H)} \rightarrow \pi^*_{(Bz)}$
E	289.57	289.3	Cp, Bz, Ph C $1s_{(C-H)} \rightarrow \sigma^*_{(C-H)}$ Bz C $1s_{(C-H),\ (Csub)} \rightarrow \pi^*_{(Bz)}$ Bz, Ph C $1s_{(Csub)} \rightarrow \sigma^*_{(C-S)}$ Ph C $1s_{(C-H),\ (Csub)} \rightarrow \pi^*_{(Ph)}$	289.2	Bz C $1s_{(Csub)} \rightarrow \pi^*_{(Bz)}$

similar to the spectrum of PPS, with a slight difference in relative intensity between features A/A′ and C/D/E. The spectrum of PPS−Fe(Cp) film irradiated with Hg-arc lamp in vacuum for 25 min (method 3) leads to similar spectral features as that obtained after 1 min irradiation with unmonochromatized synchrotron light in vacuum (data not shown).

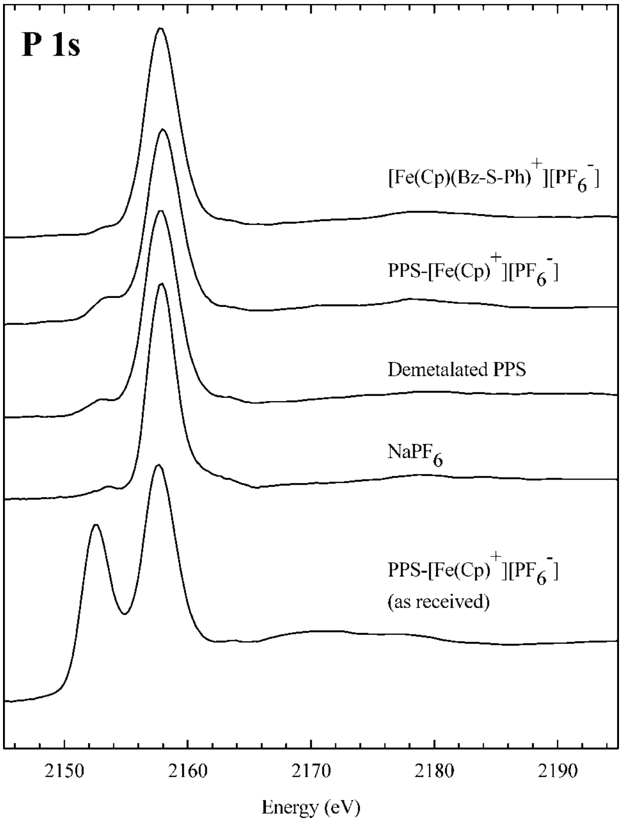

Figure 4. Phosphorus 1s edge NEXAFS spectra of the [(Cp)Fe(Bz-S-Ph)$^+$][PF$_6^-$] monomer (deposited on a copper metal substrate), a PPS−[Fe(Cp)$^+$][PF$_6^-$] film (cast from a filtered DMF solution on gold-coated silicon), PPS prepared by solution photolytic demetalation (supported by carbon tape), NaPF$_6$ powder (deposited on copper metal), and the as-received PPS−[Fe(Cp)$^+$][PF$_6^-$] powder (unfiltered; supported by carbon tape). The spectra have been offset by a constant for clarity.

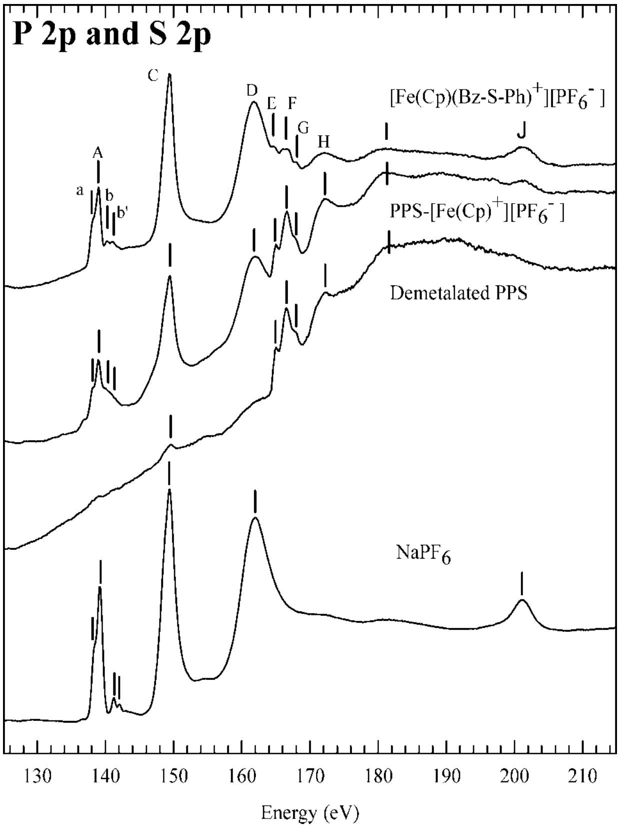

Figure 5. Phosphorus 2p and sulfur 2p NEXAFS spectra of [(Cp)Fe(Bz-S-Ph)$^+$][PF$_6^-$] monomer (deposited on copper metal), PPS−[Fe-(Cp)$^+$][PF$_6^-$] film (cast from filtered DMF solution onto gold-coated silicon), PPS prepared by solution photolytic demetalation (deposited onto copper metal), and NaPF$_6$ powder (deposited on copper metal). The spectra have been offset by a constant for clarity.

Table 4. Transition Energies (eV) and Assignment for Phosphorus 2p and Sulfur 2p NEXAFS Spectra of the $[(Cp)Fe(Bz\text{-}S\text{-}Ph)^+][PF_6^-]$ Monomer, the Metalated Polymer, $PPS-[Fe(Cp)^+][PF_6^-]$, the Demetalated Polymer, PPS, Prepared by Solution Demetalation, and $NaPF_6$

peak labels	$[(Cp)Fe(Bz\text{-}S\text{-}Ph)^+][PF_6^-]$	$PPS-[Fe(Cp)^+][PF_6^-]$	PPS (+ PF_6^-residue)	$NaPF_6$	assignment
a′		136.99		136.52	P 2p
a	138.18	138.18		138.28	P 2p
A	139.04	139.04	139.04	139.14	P 2p
b	140.33	140.5		141.26	P 2p
b′	141.08			142.12	P 2p
C	149.42	149.41	149.58	149.42	P 2p
D	161.85	162.02	162.2	162.02	P 2p
E	164.65	165.11	165.08		S $2p_{3/2}$
F	166.51	166.69	166.63		S $2p_{3/2}$ and S $2p_{1/2}$
G	167.95	167.9	167.8		S $2p_{3/2}$ and S $2p_{1/2}$
H	172.23	172.41	172.41		S $2p_{3/2}$ and S $2p_{1/2}$
I	180.8	180.9	181		
J	201.32	201.32		201.30	P 2s

4. Discussion

4.1. Characterization of Metalated and Demetalated Polymers. *4.1.1. Iron 2p Edge NEXAFS Spectra.* The iron 2p spectrum of $PPS-Fe(Cp)^+][PF_6^-]$ (Figure 1) is assigned here with the aid of the assignment of $[(Cp)Fe(Bz\text{-}S\text{-}Ph)^+][PF_6^-]$ monomer spectrum presented previously.[26] The main features A, B, and C are assigned to the following transitions: A: iron $2p_{3/2} \rightarrow$ Fe 3d $/\pi^*_{(Bz/Cp)}$; B: iron $2p_{3/2} \rightarrow \pi^*_{(Bz)}$/Fe 3d; and C: iron $2p_{3/2} \rightarrow \pi^*_{(Cp)}$/Fe 3d, respectively (see Table 2). Shoulders s observed on low-energy side of feature A in the $PPS-[Fe(Cp)^+][PF_6^-]$ spectrum are associated with the radiation sensitivity of the metalated polymer. Similar features were obtained during the X-ray radiation exposure study of (η^6-benzene)(η^5-cyclopentadienyl)iron(II) hexafluorophosphate, presented previously.[26]

The iron 2p NEXAFS spectrum of PPS (+ iron residue) confirms the presence of iron species trapped in the demetalated polymer. Significant differences are observed between the spectrum of PPS (+ iron residue) and $PPS-[Fe(Cp)^+][PF_6^-]$, indicating that these iron species are different from iron pendant moieties that might still be present in irradiated polymer due to incomplete photolysis, e.g. Fe(Cp). A tentative of identification of these iron species is presented below; a schematic of this process is presented in Scheme 2.

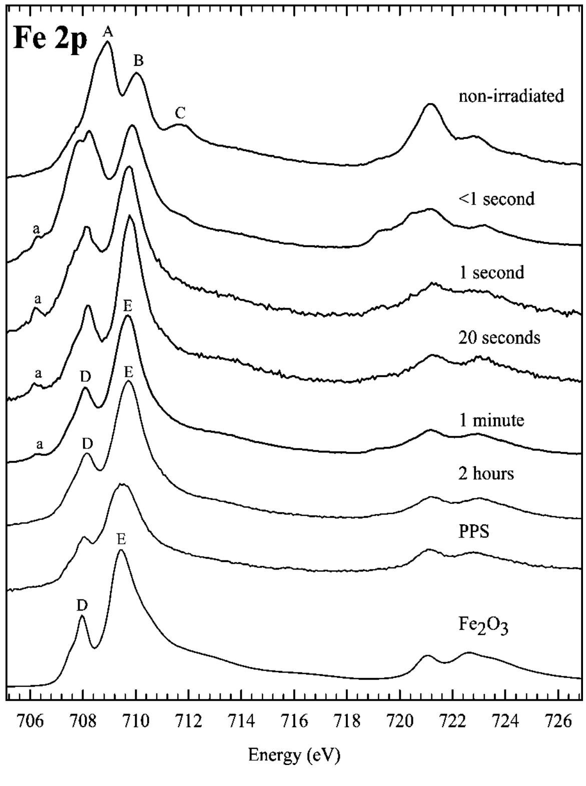

Figure 6. Iron 2p edge NEXAFS spectra of $PPS-[Fe(Cp)^+][PF_6^-]$ film (cast from filtered DFM solution onto gold-coated silicon), before irradiation and after irradiation in air with the Hg-arc lamp (method 1). This is compared to PPS prepared by solution photolytic demetalation (deposited onto indium metal) and Fe_2O_3 (deposited onto indium metal). The spectra have been offset by a constant for clarity.

Table 5. Transition Energies (eV) for Iron 2p NEXAFS Spectra of the Metalated Polymer Films, $PPS-[Fe(Cp)^+][PF_6^-]$, Demetalated Using Methods 1 and 2, and Fe_2O_3

peak labels	$PPS-[Fe(Cp)^+][PF_6^-]$ UV exposure method 1	$PPS-[Fe(Cp)^+][PF_6^-]$ UV exposure method 2	Fe_2O_3
A	706.25		
F		707.81	
D	708.11		707.97
A			
E	709.68		709.45
B			
G		710.21	
H		711.48	
C			
		719.5	
	721.1	721.1	721.1
	722.8		722.6
		723.4	

The inconsistencies observed between the spectra recorded from $PPS-[Fe(Cp)^+][PF_6^-]$ film (prepared by casting filtered solutions of the compounds) and as-received $PPS\text{-}[Fe(Cp)^+][PF_6^-]$ powder confirm the presence of iron containing residues in the powder polymer sample before demetalation. These results demonstrate the sensitivity of NEXAFS to these iron impurities and the importance of the solution/filtration preparation method for preparing appropriate polymers for controlled photolysis studies.

4.1.2. C 1s Edge NEXAFS Spectra. The assignment of the metalated and demetalated polymer spectra (Figure 3) were made with the help of the assignment of $[(Cp)Fe(Bz\text{-}S\text{-}Ph)^+][PF_6^-]$ spectrum.[26] Feature A is assigned to transition from Cp ring carbon atoms to Fe 3d orbitals mixed with Cp ligand π^* MOs and from nonsubstituted phenyl carbon atoms to phenyl π^* MOs (see Table 3). The higher energy shoulder A′ is assigned to transition from the carbon 1s orbitals on the unsubstituted benzene atom sites (C−H) to Fe 3d orbitals mixed with benzene π^* MOs. Shoulder B is assigned to transition from substituted (C−R) and nonsubstituted (C−H) benzene carbon atoms to benzene π^* MOs mixed with Fe 3d orbital; feature C is assigned to a transition from Cp carbon atoms to Cp π^* MO. In the spectrum of PPS, the absence of feature B and the decrease in intensity of peak C is consistent with the removal of Fe(Cp) moiety in the demetalated polymer.

4.1.3. Phosphorous 1s Edge NEXAFS Spectra. The phosphorus 1s spectra of $[(Cp)Fe(Bz\text{-}S\text{-}Ph)^+][PF_6^-]$, $PPS-[Fe(Cp)^+][PF_6^-]$ film, and PPS (+ PF_6^- residue) (Figure 4) are similar to the spectrum of $NaPF_6$, confirming the presence of PF_6^- as the only phosphorus-containing species in the monomer and the polymers, including the demetalated polymer. The presence of an intense feature at 2152.64 eV in the spectrum of PPS−[Fe(Cp)$^+$][PF_6^-] recorded from as received powder sample indicates the presence of phosphorus species other than PF_6^- in nonfiltered sample.

Previous studies performed on aging of PF_6^--doped polythiophenes conducting polymers show the formation of X_3PO_4, POF_3, and PF_5 species due to thermal stress.[35,36] Phosphorus 1s NEXAFS examination of the thermally aged doped polymers indicated the presence of a single peak at 2152.4 eV associated with the formation of X_3PO_4 species such as H_3PO_4.[35] The presence of moisture during sample storage was reported to contribute to the degradation of PF_6^- into POF_3, H_3PO_3, and H_3PO_4.[36] Also, strong absorption features have been reported at similar energy in the spectra of various PO_4 species.[37]

The low-energy peak (2152.64 eV) observed in the spectrum of as-received PPS−[Fe(Cp)$^+$][PF_6^-] powder sample is associated here with the presence of phosphorus oxides species that is removed by the solution/filtration process. The presence of such impurities may be the result of sample aging and/or moisture sensitivity of the metalated polymer and demonstrated the effectiveness and the importance of the solution/filtration preparation method for preparing suitable thin films from the synthesized polymers. Note that, among the various phosphorus species that may form due to sample aging and storage, some could have a vapor pressure too high to be detected during measurements under high vacuum, preventing us from proposing an exhaustive list of all species that may form. The presence of PF_6^- in demetalated polymer (PPS) is somewhat surprising since one would expect all counterions to be removed after photolysis of iron−Cp moieties and purification of demetalated polymer; its presence indicates that some countercation must be retained in the demetalated polymer. As PF_6^- can be used as a dopant in organic semiconductors to enhance conducting properties of the materials,[36] the presence of PF_6^- trapped in PPS may therefore be of some interest for potential application of PPS as conducting materials.

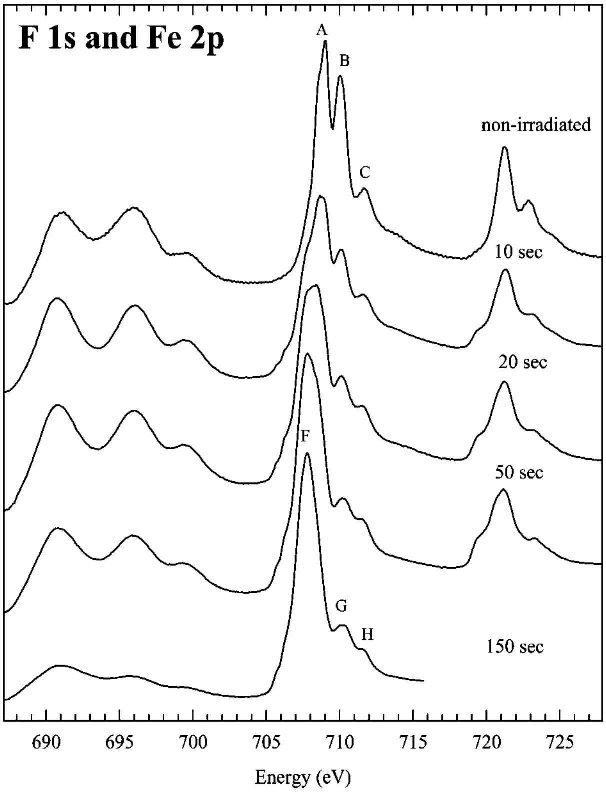

Figure 7. Fluorine 1s and iron 2p NEXAFS spectra of PPS−[Fe(Cp)$^+$][PF_6^-] film (cast from a filtered DMF solution onto gold-coated silicon, before irradiation and after irradiation in vacuum with unmonochromatized synchrotron radiation ("white light"; method 2). The spectra have been offset by a constant for clarity.

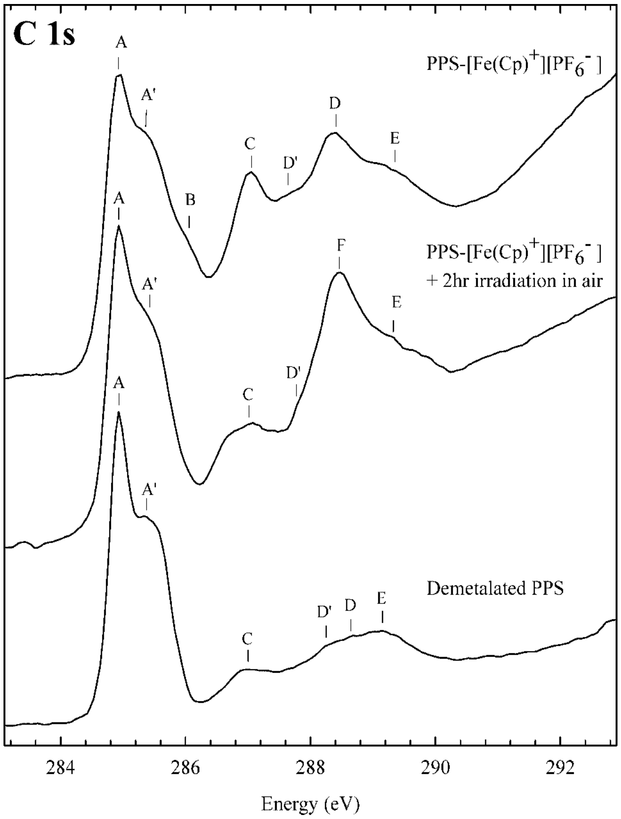

Figure 8. Carbon 1s edge NEXAFS spectra of PPS−[Fe(Cp)$^+$][PF_6^-] film (cast from filtered DMF solution onto gold-coated silicon), before irradiation and after 2 h irradiation in air using the Hg-arc lamp (method 1). These spectra are compared to that of demetalated PPS (prepared by solution photolytic demetalation and cast onto indium metal). The spectra have been offset by a constant for clarity.

4.1.4. Phosphorous 2p Edge and Sulfur 2p Edge NEXAFS Spectra. The proximity of the phosphorus 2p and sulfur 2p absorption edges allows for rationalization of the relative amount of phosphorus and sulfur atoms present in each compound (Figure 5). The decrease in phosphorus 2p resonances intensity observed between [(Cp)Fe(Bz-S-Ph)$^+$][PF_6^-] and PPS-[Fe(Cp)$^+$][PF_6^-] spectra is due to a lower phosphorus/sulfur ratio in the polymer (1:3) than in the monomer (1:1). The weak features observed below 164 eV in PPS spectrum confirm the presence of PF_6^- trapped into demetalated polymer. This is consistent with our interpretation of phosphorus 1s edge NEXAFS spectra. Moreover, we can notice that only a very small amount of PF_6^- remains trapped in PPS.

4.2. Photolytic Studies. *4.2.1. Iron 2p Edge NEXAFS Spectra.* The photolytic study performed in air on PPS−[Fe(Cp)$^+$][PF_6^-] films (Figure 6) confirms the high UV sensitivity of metalated polymer. The presence of a low-energy narrow feature (a) suggests the formation of a low-spin ferric species ($3d^5$) such as ferrocenium.[38−41] The absence of feature a from the spectrum of the PPS−[Fe(Cp)$^+$][PF_6^-] film after 2 h of irradiation indicates that this low-spin $3d^5$ iron species is likely an intermediate in the photolytic process. The similarities between the spectra of the 2 h irradiated PPS−[Fe(Cp)$^+$][PF_6^-] film and PPS (containing iron residue) suggests that the same nonvolatile iron species is present in both samples.

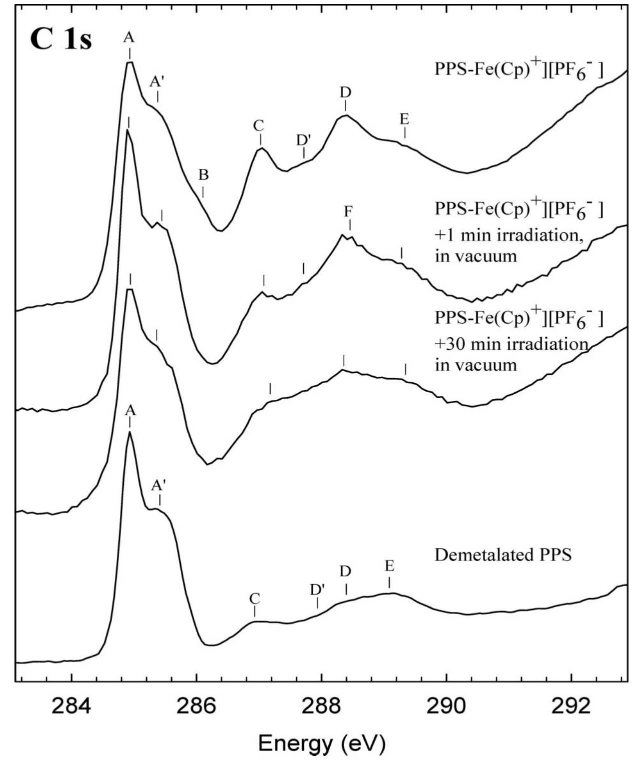

Figure 9. Carbon 1s edge NEXAFS spectra of PPS$-$[Fe(Cp)$^+$][PF$_6^-$] film (cast from filtered DMF solution onto gold-coated silicon), before irradiation and after irradiation in vacuum using unmonochromatized synchrotron light ("white light", method 2). These spectra are compared to that of demetalated PPS (prepared by solution photolytic demetalation and cast onto indium metal). The spectra have been offset by a constant for clarity.

Table 6. Transition Energies (eV) and Assignment for Carbon 1s NEXAFS Spectra of the Metalated Polymer Film, PPS$-$[Fe(Cp)$^+$][PF$_6^-$], Demetalated Using Methods 1 and 2

	PPS$-$[Fe(Cp)$^+$][PF$_6^-$]	
peak labels	method 1	method 2
A	284.94	284.94
A′	285.36	285.36
C	287	287.1
D′	287.79	
D		288.36
F	288.47	
E	289.3	289.2

The iron 2p spectrum of iron oxide (Fe$_2$O$_3$) is presented at the bottom of Figure 6. Similar spectra have been also reported for series of other ferric high-spin species.[38,42] In the case of PPS$-$[Fe(Cp)$^+$][PF$_6^-$] film, the range of possible low-spin iron species that could form upon irradiation in air is limited, unlike in solution where solvent molecules can participate in photolysis. The identification of the iron compound present in the irradiated PPS$-$[Fe(Cp)$^+$][PF$_6^-$] film as iron oxide is quite sensible. Fe$_2$O$_3$ is one of many iron oxide compounds and exists mainly in two forms, α-Fe$_2$O$_3$ (hematite) or γ-Fe$_2$O$_3$ (maghemite). The iron 2p spectrum of Fe$_2$O$_3$ presented Figure 6 was recorded from a mixture of both forms. Iron 2p spectra of pure α-Fe$_2$O$_3$ and γ-Fe$_2$O$_3$ have been reported by Paterson et al.[43] The authors show that a distinctive energy splitting between the two features observed in the iron 2p$_{3/2}$ edge spectra can be used to distinguish between the two forms: specifically a 1.55 eV splitting for α-Fe$_2$O$_3$ and 1.30 eV splitting for γ-Fe$_2$O$_3$. The energy splitting reported between features D and E in the iron 2p spectrum of 2 h irradiated PPS$-$[Fe(Cp)$^+$][PF$_6^-$] film and PPS (+ iron residue) is 1.57 and 1.47 eV, respectively, suggesting the formation of α-Fe$_2$O$_3$, which is the most stable phase of Fe$_2$O$_3$, in the irradiated film and perhaps a mixture of α and β phases in the solution demetalated PPS polymer.[44] To confirm the presence of α-Fe$_2$O$_3$ in demetalated polymers, we attempted to record Raman spectra of PPS$-$[Fe(Cp)$^+$][PF$_6^-$] film irradiated in air and PPS. However, the concentration of iron species present in both samples was below our detection limits.

The photolytic studies performed in vacuum using unmonochromatized synchrotron light and Hg-arc lamp (Figure 7) indicate the presence of iron species other than Fe$_2$O$_3$ in the irradiated films. Iron 2p NEXAFS spectra recorded from irradiated films show similarities with spectra of ferrous 3d^6 high-spin species.[38,45,46] Formation of iron species with a lower oxidation state upon irradiation in vacuum is consistent with the absence of oxygen in vacuum.

Note that in a previous study of metal arene compounds by NEXAFS spectroscopy iron 2p and carbon 1s spectra of poly(pheny ether) with iron moieties (or PPO$-$[Fe(Cp)$^+$][PF$_6^-$]) were reported and assigned.[26] A photolytic study, using method 1, has been performed on PPO$-$[Fe(Cp)$^+$][PF$_6^-$] and leads to similar results than for PPS$-$[Fe(Cp)$^+$][PF$_6^-$]; i.e., in both cases formation of Fe$_2$O$_3$ takes place (see Supporting Information, Figure S1).

4.2.2. Carbon 1s Edge NEXAFS Spectra. The spectrum of PPS$-$[Fe(Cp)$^+$][PF$_6^-$] film (Figures 8 and 9) shows clear information on the chemical changes induced by radiation. In the spectrum of PPS$-$[Fe(Cp)$^+$][PF$_6^-$] irradiated in vacuum (Figure 9), feature B is assigned to a benzene carbon $1s_{(C-H)(Csub)} \rightarrow \pi^*_{(Bz\text{-}S)}$/Fe 3d transition and feature C to the Cp carbon $1s_{(C-H)} \rightarrow \pi^*_{(Cp)}$/Fe 3d transition. In the spectrum recorded from the 1 min irradiated PPS$-$[Fe(Cp)$^+$][PF$_6^-$] film, the intensity of both features B and C decreases noticeably. This is consistent

Scheme 2. Schematic of the Expected Photolysis Reaction of PPS$-$[Fe(Cp)$^+$][PF$_6^-$], in Air, To Form PPS[a]

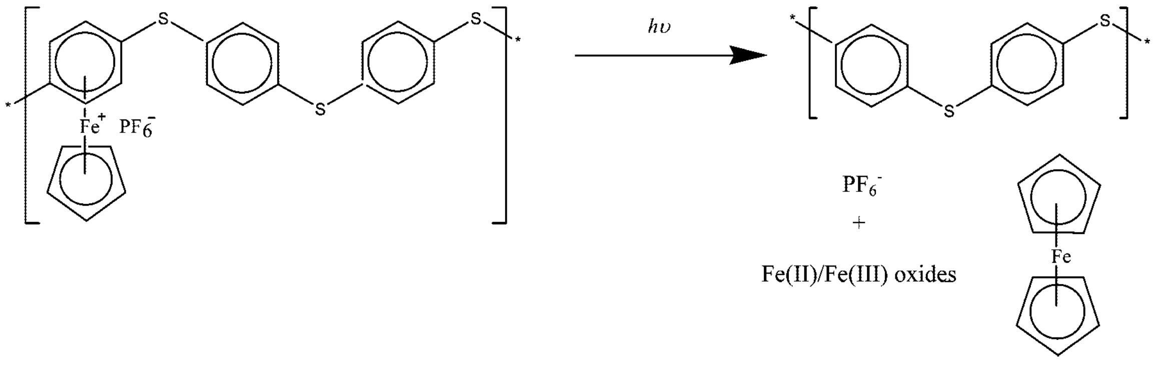

[a] The FeCp fragment, cleaved by photolysis, is believed to form volatile ferrocene and Fe(II)/Fe(III) oxides; a small amount of the PF$_6^-$ counterion remains in the irradiated polymer.

with the decoordination of the Fe(Cp) moieties upon UV irradiation. The presence of an intense feature F observed in the spectra of PPS−$[Fe(Cp)^+][PF_6^-]$ films irradiated in air (Figure 8) and in vacuum (Figure 9) and its absence in the spectrum of PPS suggest the presence of carbon containing compounds in the irradiated film that are not contained in solution demetalated PPS. Note that such compounds may have been removed from PPS during the extraction of the polymer following the photolysis of the metalated polymer in solution. As observed for the solution filtered PPS−$[Fe(Cp)^+][PF_6^-]$ polymer, processing of the metalated or demetalated polymer is expected to lead to compositional differences.

Note that for the irradiation in vacuum the final products, as identified by iron 2p and carbon 1s NEXAFS spectra, are the same regardless of the source of UV used. This suggests that in solid state the photolytic process is independent of the wavelength of the radiation used, unlike for the photolytic process in solution.

5. Conclusion

Our study of poly(pheny thioether) polymer with pendant iron moieties by NEXAFS spectroscopy reveals valuable information on the stability, composition, and structure of these complexes —material which could not be accessible by other techniques. Great sensitivity in solid state to UV and X-rays of the metalated polymer was found to lead to decoordination of the iron moieties, unlike the monomers which require high radiation dose as indicated previously.[26] Further UV irradiation of metalated poly(phenyl thioether) polymer leads to complete removal of iron moieties and formation of Fe_2O_3, which remain trapped in very small quantities inside purified demetalated poly(phenyl thioether) polymer. The concentration in oxygen was observed to play an important role in controlling the oxidation state of the iron species formed during the photolytic process. The Fe_2O_3-doped poly(phenyl thioether) polymer was also found to contain small amounts of PF_6^-. Storage conditions such as temperature and moisture appears to affect the longevity of the metalated polymer.

Acknowledgment. This work is supported by the Natural Sciences and Engineering Research Council (NSERC), the Canadian Foundation for Innovation (CFI), and the University of Saskatchewan. Experiments were performed at the Canadian Light Source (CLS) and the Synchrotron Radiation Center (SRC; University of Wisconsin—Madison). The CLS is supported by NSERC, the National Research Council (NRC), the Canadian Institutes of Health Research (CIHR), and the University Of Saskatchewan. The SRC is supported by the National Science Foundation under Award DMR-0537588. At the SRC, beamlines of the Canadian Synchrotron Radiation Facility (CSRF) were used; these were funded by NRC, NSERC, the Ontario Centre for Materials Research (OCMR), and the University of Western Ontario. We thank R. Blyth and T. Regier for their help on the SGM beamline.

Supporting Information Available: Iron 2p edge NEXAFS spectra of $[Fe(Cp)(Cl\text{-}Bz\text{-}O))_2\text{-}Ph)^{2+}][PF_6^-]$ and PPO−$[Fe(Cp)^+]$-$[PF_6^-]$. This material is available free of charge via the Internet at http://pubs.acs.org.

References and Notes

(1) Manners, I. *Science* **2001**, *294*, 1664–1666.

(2) Abd-El-Aziz, A. S.; Manners, I. *J. Inorg. Organomet. Polym. Mater.* **2005**, *15*, 157–195.

(3) Hudson, R. D. A. *J. Organomet. Chem.* **2001**, *637−639*, 47–69.

(4) Manners, I. *Synthetic Metal-Containing Polymers*; Wiley-VCH: Weinheim, 2004.000

(5) Abd-El-Aziz, A. S.; De Denus, C. R.; Zaworotko, M. J.; MacGillivray, L. R. *J. Chem. Soc., Dalton Trans.* **1995**, 3375–3393.

(6) Abd-El-Aziz, A. S.; Todd, E. K.; Epp, K. M. *J. Inorg. Organomet. Polym.* **1998**, *8*, 127–133.

(7) Abd-El-Aziz, A. S.; De Denus, C. R.; Todd, E. K.; Bernardin, S. A. *Macromolecules* **2000**, *33*, 5000–5005.

(8) Abd-El-Aziz, A. S.; Todd, E. K.; Ma, G. Z. *J. Polym. Sci., Part A: Polym. Chem.* **2001**, *39*, 1216–1231.

(9) Roloff, A.; Meier, K.; Riediker, M. *Pure Appl. Chem.* **1986**, *58*, 1267–1272.

(10) Gill, T. P.; Mann, K. R. *Inorg. Chem.* **1980**, *19*, 3007–3010.

(11) Gill, T. P.; Mann, K. R. *Inorg. Chem.* **1983**, *22*, 1986–1991.

(12) Karatsu, T.; Shibuki, Y.; Miyagawa, N.; Takahara, S.; Kitamura, A.; Yamaoka, T. *J. Photochem. Photobiol. A: Chem.* **1997**, *107*, 83 91.

(13) Nesmeyanov, A. N.; Vol'kenau, N. A.; Shilovtseva, L. S. *Dokl. Akad. Nauk SSSR* **1970**, *190*, 857–859.

(14) Schrenk, J. L.; Palazzotto, M. C.; Mann, K. R. *Inorg. Chem.* **1983**, *22*, 4047–4049.

(15) McNair, A. M.; Schrenk, J. L.; Mann, K. R. *Inorg. Chem.* **1984**, *23*, 2633–2640.

(16) Mann, K. R.; Blough, A. M.; Schrenk, J. L.; Koefod, S. R.; Freedman, D. A.; Matachek, J. R. *Pure Appl. Chem.* **1995**, *67*, 95–101.

(17) Jakúbek, V.; Lees, A. J. *Chem. Commun.* **1999**, 1631–1632.

(18) Román, E.; Barrera, M.; Hernández, S. *J. Chem. Soc., Perkin Trans. 2* **1988**, 939–942.

(19) Boyd, D. C.; Bohling, D. A.; Mann, K. R. *J. Am. Chem. Soc.* **1985**, *107*, 1641–1644.

(20) Chrisope, D. R.; Park, K. M.; Schuster, G. B. *J. Am. Chem. Soc.* **1989**, *111*, 6195–6201.

(21) Turner, C. A.; Ding, W.; Amster, I. J.; Kutal, C. *Coord. Chem. Rev.* **2002**, *229*, 9–16.

(22) Ding, W.; Johnson, K. A.; Kutal, C.; Amster, I. J. *Anal. Chem.* **2003**, *75*, 4624–2630.

(23) Jakúbek, V.; Lees, A. J. *Inorg. Chem.* **2000**, *39*, 5779–5786.

(24) Chan, W. Y.; Clendenning, S. B.; Berenbaum, A.; Lough, A. J.; Aouba, S.; Ruda, H. E.; Manners, I. *J. Am. Chem. Soc.* **2005**, *127*, 1765–1772.

(25) Liu, K.; Ho, C.-L.; Aouba, S.; Zhao, Y.-Q.; Lu, Z.-H.; Petrov, S.; Coombs, N.; Dube, P.; Ruda, H. E.; Wong, W.-Y.; Manners, I. *Angew. Chem., Int. Ed.* **2008**, *47*, 1255–1259.

(26) Otero, E.; Shipman, P. O.; Abd-El-Aziz, A. S.; Urquhart, S. G. *Organometallics* **2008**, 000. submitted.

(27) Tan, K. H.; Bancroft, G. M.; Coatsworth, L. L.; Yates, B. W. *Can. J. Phys.* **1982**, *60*, 131.

(28) Regier, T.; Paulsen, J.; Wright, G.; Coulthard, I.; Tan, K.; Sham, T. K.; Blyth, R. I. R. In *Synchrotron Radiation Instrumentation: Ninth International Conference on Synchrotron Radiation Instrumentation*; Choi, J. Y., Rah, S., Eds.; American Institute of Physics: Daegu, Korea, 2006; pp 473−476.

(29) Yang, B. X.; Middleton, F. H.; Olsson, B. G.; Bancroft, G. M.; Chen, J. M.; Sham, T. K.; Tan, K.; Wallace, D. J. *Rev. Sci. Instrum.* **1992**, *63*, 1355–1358.

(30) Otero, E.; Wilks, R.; Regier, T.; Blyth, R. I. R.; Moewes, A.; Urquhart, S. G. *J. Phys. Chem. A* **2008**, *112*, 624–634.

(31) Sutherland, D. G. J.; Kasrai, M.; Bancroft, G. M.; Liu, Z. F.; Tan, K. H. *Phys. Rev. B* **1993**, *48*, 14989–15001.

(32) Li, D.; Bancroft, G. M.; Kasrai, M.; Fleet, M. E.; Secco, R. A.; Feng, X. H.; Tan, K. H.; Yang, B. X. *Am. Mineral.* **1994**, *79*, 622–632.

(33) Urquhart, S. G.; Hitchcock, A. P.; Priester, R. D.; Rightor, E. G. *J. Polym. Sci., Part B: Polym. Phys.* **1995**, *33*, 1603–1620.

(34) Engemann, C.; Kohring, G.; Pantelouris, A.; Hormes, J.; Grimme, S.; Peyerimhoff, S. D.; Clade, J.; Frick, F.; Jansen, M. *Chem. Phys.* **1997**, *221*, 189–198.

(35) Winter, I.; Hormes, J.; Hiller, M. *Nucl. Instrum. Methods Phys. Res. B* **1995**, *97*, 287–291.

(36) Gozet, T.; Hacaloglu, J. *Polym. Int.* **2004**, *53*, 2162–2168.

(37) Brandes, J. A.; Ingall, E.; Paterson, D. *Marine Chem.* **2007**, *103*, 250–265.

(38) Wasinger, E. C.; De Groot, F. M. F.; Hedman, B.; Hodgson, K. O.; Solomon, E. I. *J. Am. Chem. Soc.* **2003**, *125*, 12894–12906.

(39) Hocking, R. K.; Wasinger, E. C.; De Groot, F. M. F.; Hodgson, K. O.; Hedman, B.; Solomon, E. I. *J. Am. Chem. Soc.* **2006**, *128*, 10442–10451.

(40) Otero, E.; Kosugi, N.; Urquhart, S. G. Manuscript in preparation.

(41) Otero, E. PhD Thesis, University of Saskatchewan, Saskatoon, **2008**.

(42) Vinogradov, A. S.; Preobrajenski, A. B.; Krasnikov, S. A.; Chasse, T.; Szargan, R.; Knop-Gericke, A.; Schlogl, R.; Bressler, P. *Surf. Rev. Lett.* **2002**, *9*, 359–364.

(43) Paterson, J. H.; Krivanek, O. L. *Ultramicroscopy* **1990**, *32*, 319–325.

(44) Holleman, A. F.; Wiberg, E. *Inorganic Chemistry*; Academic Press: Berlin, 2001.000

(45) Crocombette, J. P.; Pollak, M.; Jollet, F.; Thromat, N.; Gautier-Soyer, M. *Phys. Rev. B* **1995**, *52*, 3143–3150.

(46) Regan, T. J.; Ohldag, H.; Stamm, C.; Nolting, F.; Lüning, J.; Stöhr, J.; White, R. L. *Phys. Rev. B* **2001**, *64*, 214422.

MA801826P